Trio's Rho-specific GEF domain is the missing $G\alpha_q$ effector in *C. elegans*

Stacey L. Williams,[1] Susanne Lutz,[2] Nicole K. Charlie,[1] Christiane Vettel,[2] Michael Ailion,[3] Cassandra Coco,[4] John J.G. Tesmer,[4] Erik M. Jorgensen,[3] Thomas Wieland,[2] and Kenneth G. Miller[1,5]

[1]Program in Molecular, Cell, and Developmental Biology, Oklahoma Medical Research Foundation, Oklahoma City, Oklahoma 73104, USA; [2]Institute of Experimental and Clinical Pharmacology, Medical Faculty Mannheim, University of Heidelberg, D-68169 Mannheim, Germany; [3]Department of Biology, Howard Hughes Medical Institute, University of Utah, Salt Lake City, Utah 84112, USA; [4]Department of Pharmacology, Life Sciences Institute, University of Michigan, Ann Arbor, Michigan 48109, USA

The $G\alpha_q$ pathway is essential for animal life and is a central pathway for driving locomotion, egg laying, and growth in *Caenorhabditis elegans*, where it exerts its effects through EGL-8 (phospholipase Cβ [PLCβ]) and at least one other effector. To find the missing effector, we performed forward genetic screens to suppress the slow growth and hyperactive behaviors of mutants with an overactive $G\alpha_q$ pathway. Four suppressor mutations disrupted the Rho-specific guanine-nucleotide exchange factor (GEF) domain of UNC-73 (Trio). The mutations produce defects in neuronal function, but not neuronal development, that cause sluggish locomotion similar to animals lacking EGL-8 (PLCβ). Strains containing null mutations in both EGL-8 (PLCβ) and UNC-73 (Trio RhoGEF) have strong synthetic phenotypes that phenocopy the arrested growth and near-complete paralysis of $G\alpha_q$-null mutants. Using cell-based and biochemical assays, we show that activated *C. elegans* $G\alpha_q$ synergizes with Trio RhoGEF to activate RhoA. Activated $G\alpha_q$ and Trio RhoGEF appear to be part of a signaling complex, because they coimmunoprecipitate when expressed together in cells. Our results show that Trio's Rho-specific GEF domain is a major $G\alpha_q$ effector that, together with PLCβ, mediates the $G\alpha_q$ signaling that drives the locomotion, egg laying, and growth of the animal.

[*Keywords*: $G\alpha_q$; Trio; Rho; phospholipase Cβ; *C. elegans*]

Supplemental material is available at http://www.genesdev.org.

Received July 10, 2007; revised version accepted August 31, 2007.

The $G\alpha_q$ pathway is one of the major routes through which receptor-generated signals affect the state and function of neurons and other cells (Hubbard and Hepler 2006). Like other members of the family of heterotrimeric G proteins, $G\alpha_q$ becomes activated when a ligand, such as a neurotransmitter, binds to a $G\alpha_q$-coupled receptor. This causes the receptor to act as a guanine-nucleotide exchange factor (GEF) that converts $G\alpha_q$ from its inactive GDP-bound state into its active GTP-bound state and facilitates its dissociation from the βγ subunits of the G protein (Gilman 1987; Hepler and Gillman 1992; Neer 1995; Bourne 1997).

In their activated state, the Gα and βγ subunits activate specific effector proteins that ultimately change the state of the cell. Thus, to understand how a G protein pathway affects a cell's functional state, it is crucial to identify all of the effector proteins through which the G protein acts. Early pioneering studies of the $G\alpha_q$ pathway revealed that phospholipase Cβ (PLCβ) is an important $G\alpha_q$ effector protein (Smrcka et al. 1991; Taylor et al. 1991). $G\alpha_q$-activated PLCβ cleaves the lipid PIP_2 into the small signaling molecules DAG and IP_3. More recently, there has been an emerging body of evidence definitively linking $G\alpha_q$-coupled receptors and activated $G\alpha_q$ to Rho activation, independent of effects on PLCβ (Katoh et al. 1998; Chikumi et al. 2002; Dutt et al. 2002; Vogt et al. 2003; Barnes et al. 2005; Lutz et al. 2005, 2007; Rojas et al. 2007). However, the biological significance of this newly discovered $G\alpha_q$ effector pathway has not been determined, thus leaving fundamental questions unanswered. For example, what is the relative importance of each effector pathway in the total scheme of $G\alpha_q$ signaling? Are both pathways active in the same cells at the same time, or are they specialized for different cell types or responses? Given the key role of $G\alpha_q$ signaling in many different cell types (Wilkie et al. 1991; Hubbard and Hepler 2006) and that it is essential for animal life (Brundage et al. 1996; Offermanns et al. 1998), these are important questions to answer.

[5]Corresponding author.
E-MAIL millerk@omrf.org; FAX (405) 271-3153.
Article published online ahead of print. Article and publication date are online at http://www.genesdev.org/cgi/doi/10.1101/gad.1592007.

Since the $G\alpha_q$ pathway is highly conserved in all animals (~82% identical between *Caenorhabditis elegans* and humans), genetic studies in model organisms provide a way to address the above questions. In *C. elegans* neurons, a synaptic signaling network of heterotrimeric G protein pathways, including a core $G\alpha_q$ pathway, controls synaptic activity to produce behaviors such as locomotion and egg laying (see Fig. 1 and references in legend). Under standard *C. elegans* culture conditions, animals lacking a $G\alpha_q$ pathway exhibit a larval growth arrest and strong paralysis that can be acutely rescued to wild-type levels of locomotion by applying phorbol esters, which are DAG analogs (Brundage et al. 1996; Reynolds et al. 2005). $G\alpha_q$ reduction-of-function mutants survive to become sluggish or paralyzed egg-laying-defective adults with impaired neurotransmitter release (Brundage et al. 1996; Miller et al. 1996, 1999; Hajdu-Cronin et al. 1999; Lackner et al. 1999).

Past genetic studies have shown that the *C. elegans* $G\alpha_q$ ortholog, known as EGL-30 for its egg-laying-defective phenotype, exerts its effects in part through EGL-8, which is the only neuronal PLCβ ortholog in *C. elegans* (Lackner et al. 1999; Miller et al. 1999; Bastiani et al. 2003). However, these studies all inferred at least one other $G\alpha_q$ effector pathway based on the finding that a $G\alpha_q$-null mutant is much more impaired for locomotion, egg laying, and growth than a mutant lacking EGL-8 (PLCβ) (Lackner et al. 1999; Miller et al. 1999; Bastiani et al. 2003). In this study, we used two forward genetic screen strategies to identify candidates for the missing $G\alpha_q$ effector. In so doing, we recovered mutations that disrupt the Rho-specific GEF domain of UNC-73 (Trio). Through complementary genetic, biochemical, and cell-based approaches, we show that Trio's Rho-specific GEF domain is a major $G\alpha_q$ effector that, together with PLCβ, mediates the $G\alpha_q$ signaling that drives the locomotion, egg laying, and growth of the animal. These results provide the first insights into the relative importance of the RhoGEF and PLCβ $G\alpha_q$ effector pathways in the context of a living animal.

Results

Loss-of-function mutations in Trio's Rho-specific GEF domain suppress mutants with a hyperactivated $G\alpha_q$ pathway

To identify the missing $G\alpha_q$ effector pathway in *C. elegans*, we first performed a forward genetic screen to look for mutations that enhanced the phenotypes of *egl-8* (PLCβ)-null mutants to the point that they resembled $G\alpha_q$-null mutants. Specifically, we looked for mutations that conferred wild-type or sluggish phenotypes in a wild-type background but showed strong paralysis and/or larval arrest in an *egl-8*-null background (see Materials and Methods). We carried out the screen clonally and, over 13 weekly cycles, examined enough animals to test every gene in the *C. elegans* genome an average of approximately three times for a role in the missing $G\alpha_q$ effector pathway. However, we found no clear enhancer mutations in the screen. Although this

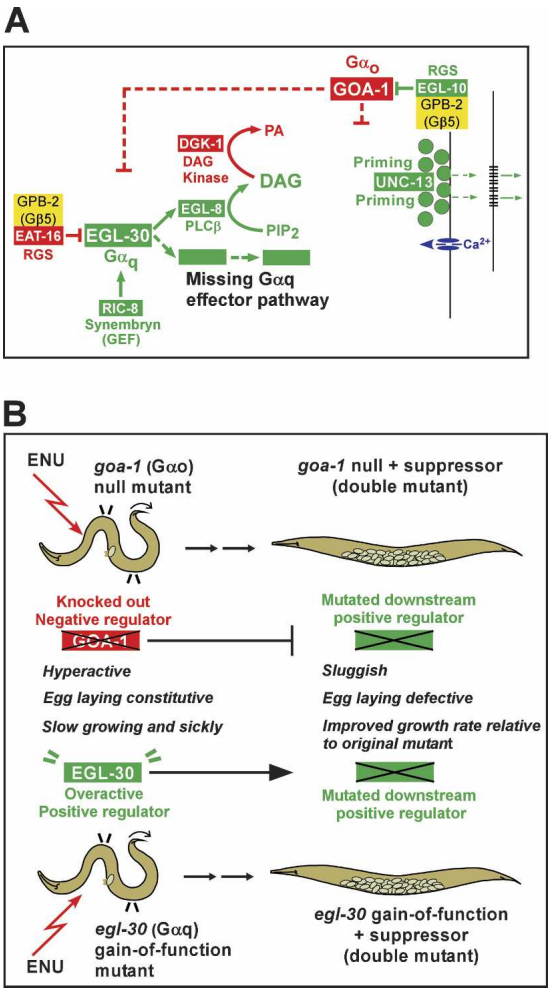

Figure 1. The missing $G\alpha_q$ effector pathway and targeted forward genetic screens for finding it. (*A*) Summary of the $G\alpha_o$ and $G\alpha_q$ pathways that drive *C. elegans* locomotion and egg laying. Solid lines indicate that direct interactions are known or likely, while dashed lines, such as the missing $G\alpha_q$ effector pathway, indicate probable missing components. The green proteins positively drive locomotion and neurotransmitter release, and reducing their function causes decreased neurotransmitter release, decreased locomotion or paralysis, and decreased egg laying. The red proteins inhibit locomotion and neurotransmitter release, and reducing their function causes increased neurotransmitter release and hyperactive behaviors. Note that the GOA-1 ($G\alpha_o$) pathway exerts its inhibitory effects in a $G\alpha_q$ pathway-dependent manner. Not shown is a third Gα pathway in this network ($G\alpha_s$) (Reynolds et al. 2005; Schade et al. 2005; Charlie et al. 2006a,b). The model is based on the following studies: Mendel et al. (1995), Segalat et al. (1995), Brundage et al. (1996), Koelle and Horvitz (1996), Hajdu-Cronin et al. (1999), Lackner et al. (1999), Miller et al. (1999, 2000), Nurrish et al. (1999), Richmond et al. (1999, 2001), Chase et al. (2001), Robatzek et al. (2001), van der Linden et al. (2001), and Bastiani et al. (2003). (*B*) Two forward genetic screen strategies for identifying the missing $G\alpha_q$ effector pathway. Both screen strategies use the mutagen ENU to suppress the slow growth and hyperactive phenotypes of mutants with an overactive $G\alpha_q$ pathway for the purpose of identifying downstream effectors.

screen was too small to ensure recovery of domain-specific mutations or reduction-of-function mutations in genes with lethal null phenotypes, it revealed that strong synthetic interactions with *egl-8* (PLCβ)-null mutants are rare, and that a simple gene knockout is probably insufficient to reveal the missing $G\alpha_q$ effector.

To continue searching for the missing $G\alpha_q$ effector pathway, we designed forward genetic screens in which we attempted to suppress or partially suppress mutants with an overactive $G\alpha_q$ pathway, with the rationale that mutations in downstream effectors would block or partially block the effects of an overactive $G\alpha_q$ pathway. To carry out these screens, we mutagenized *goa-1* ($G\alpha_o$)-null mutants as well as *egl-30* ($G\alpha_q$) gain-of-function mutants (Fig. 1B). As depicted in Figure 1A, previous genetic studies showed that GOA-1 ($G\alpha_o$) exerts its inhibitory effects in a $G\alpha_q$-pathway-dependent manner, so *goa-1*-null mutants effectively have an overactive $G\alpha_q$ pathway (Hajdu-Cronin et al. 1999; Miller et al. 1999). Both *goa-1*-null and *egl-30* gain-of-function mutants have very slow growth and hyperactive behaviors. Our genetic screens sought to suppress both of these phenotypes. This allowed us to select against nonspecific mutations, such as mutations that slow locomotion (e.g., by disrupting muscle function) without improving growth rate, and to select for mutants with a growth advantage.

After screening ENU-mutagenized lines at an estimated fivefold to 15-fold knockout coverage for the combined screens, we recovered mutants satisfying the suppression criteria and mapped the mutations to specific genes. Among other genes, we recovered mutations in expected targets such as *egl-30* ($G\alpha_q$), *egl-8* (PLCβ), and *ric-8* (GEF for $G\alpha_q$). These mutations and others will be described elsewhere. Unexpectedly, however, both of the genetic screens produced mutations with strong suppression phenotypes in the previously identified *unc-73* gene (Fig. 2A–C). For example, the *ce362* mutation improved the growth rate of the *goa-1* null more than sixfold, to a level that was 83% of the *unc-73(ce362)* single mutant (Fig. 2B). The strongest suppressor mutant from each of the screens also suppressed the locomotion rate of *goa-1*-null and *egl-30* gain-of-function mutants to a level that was similar to the sluggish locomotion rate of each *unc-73* single mutant (Fig. 2C).

UNC-73 is the *C. elegans* Trio ortholog (Steven et al. 1998). Its functions are mediated largely by two prominent GEF domains that activate small monomeric G proteins by catalyzing the transition from the inactive GDP-bound state to the active GTP-bound state. UNC-73's first GEF domain is specific for Rac GTPases (Steven et al. 1998) and the second for Rho GTPases (Fig. 3; Spencer et al. 2001). With alternative transcripts, *C. elegans* can make proteins that have the Rho-specific GEF domain but lack the Rac-specific GEF domain (Fig. 3; Steven et al. 2005). All four of our *unc-73* mutations specifically disrupt the Rho-specific GEF domain with missense mutations or a two-amino-acid deletion (Fig. 3; Supplementary Fig. 1). A previous study produced the *ev802* deletion that eliminates this domain and showed that it causes larval arrest and sluggish locomotion (Steven et al. 2005). Like *unc-73(ev802)*, our mutations confer sluggish locomotion (Fig. 3), which suggests that they are loss-of-function mutations; however, even our strongest suppressor mutant, *unc-73(ce362)*, did not exhibit larval arrest, and none of our mutants had a locomotion rate as

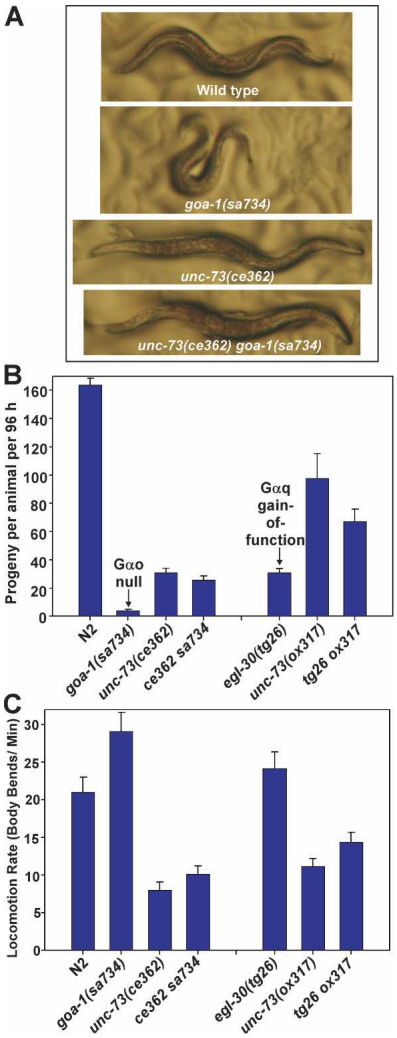

Figure 2. Mutations in *unc-73* (Trio) suppress the growth and locomotion phenotypes of mutants with a hyperactivated $G\alpha_q$ pathway. (*A*) The *unc-73(ce362)* mutation causes a striking change in the appearance of a *goa-1* ($G\alpha_o$)-null mutant. The photographs show how the *unc-73(ce362)* mutation converts a *goa-1*-null mutant from an animal with a small, thin, loopy appearance to a larger, fatter looking animal with a more relaxed posture. Compare with wild type in *top* panel. (*B*) Mutations in *unc-73* (Trio) improve the growth of mutants with a hyperactivated $G\alpha_q$ pathway. The graph depicts mean growth rates of wild type and the indicated single and double mutants. Growth rate is measured as mean number of progeny produced per animal over a 96-h period starting with newly hatched larvae. Error bars represent the standard errors of three populations of larvae. (*C*) Mutations in *unc-73* (Trio) slow the locomotion of mutants with a hyperactivated $G\alpha_q$ pathway. The graph compares locomotion rates, expressed as body bends per minute, of wild type and the indicated single and double mutants. Error bars are the standard errors of 10 animals.

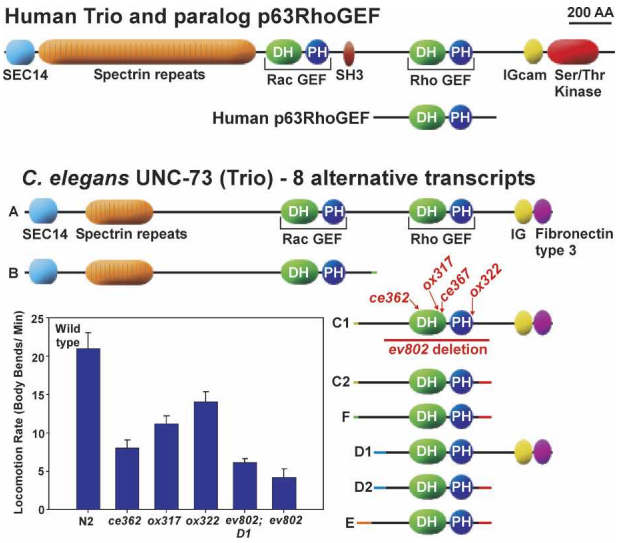

Figure 3. Four mutations that suppress mutants with an overactive $G\alpha_q$ pathway disrupt UNC-73's Rho-specific GEF domain. Shown are scale drawings comparing the domain structures of human Trio, human p63RhoGEF, and the eight alternative gene products of the *C. elegans unc-73* (Trio) locus as described by Steven et al. (2005). Red arrows indicate the sites of the four suppressor mutations that disrupt the Rho-specific GEF domain (allele names *ce362*, *ox317*, *ce367*, and *ox322*). A red line denotes the boundaries of the *ev802* deletion mutation (Steven et al. 2005). The graph compares the mean locomotion rates of wild type and the various Rho-specific GEF domain mutants, including the *ev802*-null mutant. *ev802 [D1]* is a strain containing the deletion mutation that has been rescued for its larval arrest phenotype with the D1 transcript (Steven et al. 2005). Since D1 is mainly expressed in the pharynx and egg-laying muscles (Steven et al. 2005), this strain is close to a null for UNC-73 in most of the nervous system; however, small amounts of expression in neurons driving locomotion cannot be ruled out, and there appears to be a slight improvement in locomotion rate over the *ev802* null that lacks that transgene. Error bars are the standard errors of 10 animals.

low as the *ev802* deletion mutant (Fig. 3), so all four suppressor mutations are likely to be reduction-of-function mutations but not nulls. Our molecular analysis of the mutations also suggests that at least two of the four mutations, *ox317* and *ce362*, reduce the RhoGEF function of the domain and are not unusual activating mutations. *ox317* is likely to reduce function because it is analogous to a residue in Trio's Rac-specific GEF domain that, when mutated, nearly eliminates Rac nucleotide exchange activity (Liu et al. 1998). Interestingly, our *ce362* mutant and the *ev802* deletion mutant both have significantly stronger locomotion and growth phenotypes than *ox317*, suggesting that *ox317* does not completely knock out GEF activity in vivo. As described below, the *ce362* mutation strongly reduces the function of the domain, or its ability to be activated, in cell-based and biochemical assays. Hereafter, we refer to mutants that specifically disrupt the UNC-73 Rho-specific GEF domain as *unc-73* RhoGEF mutants.

The sluggishness of unc-73 *RhoGEF mutants is caused by defects in neuronal function, not neuronal development*

All of the *unc-73* mutations that were previously isolated in forward genetic screens disrupt the animal's ability to make a functional Rac-specific GEF domain, which is found only in *unc-73*'s longer A and B transcripts; however, animals carrying mutations upstream of the short transcripts C–F can still make a functional Rho-specific GEF domain (Fig. 3; Steven et al. 2005). Mutations disrupting the A and B transcripts cause animals to be uncoordinated because of developmental defects in cell migrations, including axonal growth cone migrations (Hedgecock et al. 1987; Desai et al. 1988; Siddiqui 1990; Siddiqui and Culotti 1991; McIntire et al. 1992; Wightman et al. 1997; Steven et al. 1998). Given UNC-73's prominent role in neuronal development, we wanted to test if defects in neuronal development contribute to the sluggishness of *unc-73* RhoGEF mutants. To do this, we expressed the *unc-73e* cDNA under control of an inducible heat-shock promoter and induced its expression in adult *unc-73(ce362)* mutants, after neuronal development is complete. A 50-min heat-shock induction of the transgene rescued the locomotion rate of *unc-73(ce362)* adults to greater than wild-type levels, whereas the same heat-shock treatment slowed the locomotion rate of control strains that lacked the transgene (Fig. 4A; Supplementary Movies). We conclude that the sluggish locomotion of *unc-73* RhoGEF mutants is caused by functional, not developmental, defects.

Animals can be sluggish due to a muscle problem or a nervous system problem. To determine the extent to which neuronal defects contribute to the sluggishness of *unc-73* mutants, we transformed the *unc-73(ce362)* mutant with a transgene that expresses the *unc-73e* cDNA pan-neuronally. This transgene restored wild-type locomotion rates to the mutant (Fig. 4B). In summary, the results in Figure 4 show that the sluggishness of *unc-73* RhoGEF mutants is caused by a defect in neuronal function, and not neuronal development or muscle function.

unc-73 *RhoGEF mutants have drug sensitivities consistent with a mild deficit in ACh synaptic transmission*

Given previous findings that *egl-30* ($G\alpha_q$) and *goa-1* ($G\alpha_o$) mutants exhibit pharmacological responses that are consistent with defective regulation of ACh synaptic transmission, we sought evidence that *unc-73(ce362)* mutants have decreased release of the neuromuscular neurotransmitter ACh. For this purpose, we used an assay that measures the time course of paralysis on the acetylcholinesterase inhibitor aldicarb. Since the secreted ACh that accumulates in the presence of aldicarb is toxic, mutations that decrease or increase the rate of ACh secretion confer resistance or hypersensitivity to aldicarb, respectively (Rand and Nonet 1997). The data showed that our strongest viable *unc-73* mutant is only slightly resistant to aldicarb in this acute paralysis assay, and

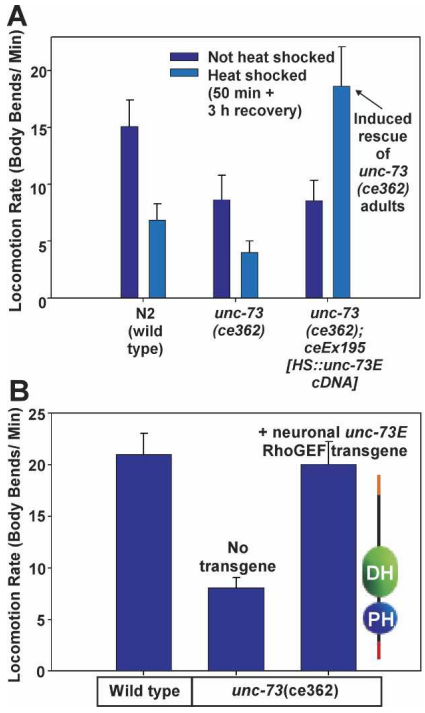

Figure 4. The sluggishness of *unc-73* RhoGEF mutants is caused by defects in neuronal function, not neuronal development. (*A*) UNC-73's RhoGEF domain functions in adults, after neuronal development is complete. Locomotion rates of control mutants compared with an *unc-73(ce362)* mutant that expresses the *unc-73* cDNA under control of an inducible heat-shock promoter. Dark-blue and light-blue bars depict mean locomotion rates of eight adults of each strain before and after a 50-min heat shock followed by a 3-h recovery period. Error bars are standard errors of the means. See also the Supplementary Movies. (*B*) UNC-73's RhoGEF domain functions in the nervous system. Mean locomotion rates, in body bends per minute, of the *unc-73(ce362)* mutant plus or minus the *ceIs39 [rab-3::unc-73e cDNA]* transgene that expresses the *unc-73e* cDNA throughout the nervous system. Error bars are standard errors of the means of 10 animals.

only at later time points in the assay (Fig. 5A). A transgene that expresses the *unc-73e* cDNA throughout the nervous system restores aldicarb sensitivity to wild-type levels in the *unc-73(ce362)* mutant background, which suggests that the mild aldicarb resistance at later time points is not due to irrelevant background mutations in the strain (Fig. 5A). In contrast, an *egl-8* (PLCβ)-null mutant assayed in parallel is resistant throughout the time course (Fig. 5A). These results argue for distinct functions of the UNC-73 RhoGEF domain and PLCβ in driving locomotion, since their similar levels of sluggishness (as shown in the next section) are not reflected in similar aldicarb sensitivities.

For unknown reasons, some mutants that are defective in neurotransmitter release are hypersensitive to the nicotinic ACh receptor agonist levamisole (Nonet et al. 1993; Miller et al. 1996). Both *egl-8* (PLCβ) mutants and our *unc-73* RhoGEF mutants are significantly hypersensitive to the paralytic effects of levamisole, and this is rescued by the transgene that expresses the *unc-73* cDNA pan-neuronally (Fig. 5B). Regardless of the explanation for the levamisole hypersensitivity, this suggests that the sluggishness and slight aldicarb resistance of *unc-73* RhoGEF mutants are not caused by reduced response of the muscle to ACh. In summary, the results in Figure 5 are consistent with *unc-73* RhoGEF mutants having only a mild deficit in ACh synaptic transmission; however, it is possible that up-regulation of the response to ACh, as reflected by the hypersensitivity, interferes with our ability to detect a strong ACh release defect by this method.

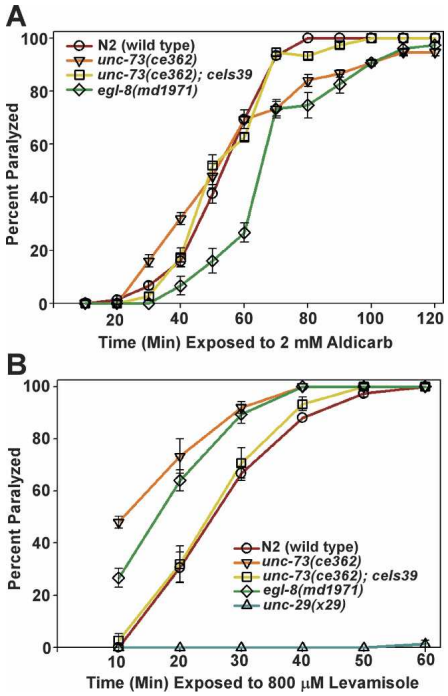

Figure 5. *unc-73* RhoGEF mutants exhibit drug sensitivities consistent with a mild deficit in ACh release. (*A*) *unc-73(ce362)* mutants exhibit delayed aldicarb-induced paralysis at later time points relative to wild type and neuronally rescued *unc-73(ce362)*. Shown are the percentage of animals that are paralyzed at various time points during incubation on a 2 mM aldicarb plate. The *ceIs39 [rab-3::unc-73e cDNA]* transgene expresses the *unc-73e* cDNA pan-neuronally. The aldicarb resistance of *egl-8(md1971)*, a probable null mutant of PLCβ (Miller et al. 1999), is significantly stronger than *unc-73(ce362)* during the first hour of exposure. Data are the means and standard errors of three trials and are representative of two independent experiments. (*B*) *unc-73(ce362)* mutants are hypersensitive to the ACh receptor agonist levamisole relative to wild type and neuronally rescued *unc-73(ce362)*. Shown are the percentage of animals that are paralyzed at various time points during incubation on an 800 μM levamisole plate. The *ceIs39 [rab-3::unc-73e cDNA]* transgene restores wild-type levamisole sensitivity to *unc-73(ce362)*. Also shown is *unc-29(x29)*, which lacks functional levamisole receptors (Gally et al. 2004) and is completely resistant to levamisole-induced paralysis. Data are the means and standard errors of three trials.

Double mutants disrupted for both PLCβ and UNC-73 RhoGEF have synthetic phenotypes resembling $G\alpha_q$ nulls

We next investigated the relationship between UNC-73 (Trio) and the $G\alpha_o$–$G\alpha_q$ signaling network. Our finding that *unc-73* RhoGEF mutants suppress mutants with an overactive $G\alpha_q$ pathway is consistent with UNC-73's RhoGEF domain acting as an effector in the $G\alpha_q$ pathway, but it is also consistent with *unc-73* mutations affecting $G\alpha_q$ pathway function indirectly. One way to test relationships within pathways is through double-mutant analysis. If UNC-73's RhoGEF domain is the missing $G\alpha_q$ effector, then a double mutant lacking both PLCβ and UNC-73 RhoGEF should have the phenotypes of a $G\alpha_q$-null mutant. That is indeed what we found. Single mutants lacking only PLCβ or only UNC-73's RhoGEF domain were similarly sluggish, but not paralyzed; however, double mutants that were null for both proteins were almost completely paralyzed and had mean locomotion rates slightly lower than, but not significantly different from, a $G\alpha_q$-null mutant (Fig. 6A; Supplementary Movies). Even the nonnull *unc-73* RhoGEF mutants *ce362* and *ox317*, when combined with PLCβ nulls, produced double mutants with locomotion rates close to a $G\alpha_q$ null (Fig. 6A). We also found that an *unc-108* mutant (also isolated in the *goa-1* suppressor screen) does not show a synthetic interaction with *egl-8*, even though it is more sluggish than the UNC-73 RhoGEF mutant (Fig. 6A). This latter result is consistent with our findings from the *egl-8* enhancer screen (described above) showing that synthetic interactions with the *egl-8* null are rare.

The *unc-73 RhoGEF; egl-8* double mutants phenocopied *egl-30* ($G\alpha_q$)-null mutants in general appearance and growth characteristics as well as locomotion. For example, due to lack of locomotion, newly hatched *egl-30* nulls and *unc-73 RhoGEF; egl-8* double nulls (hereafter referred to as "double nulls") remain folded as they were in the egg for hours after hatching (Fig. 6B; Supplementary Movies). *egl-30* nulls and the double nulls also share an early larval growth arrest phenotype under standard laboratory culture conditions (Table 1). Most arrested larvae remain alive for a week or more [75 ± 2.9% of *unc-73(ev802); egl-8(sa47)* double mutants were still alive after 10 d; $n = 3$ populations of 20 animals each]. Much of the growth arrest phenotype of the double nulls is caused by absence of the UNC-73 RhoGEF, since the *unc-73* RhoGEF-null mutant showed >50% larval growth arrest even as a single mutant, whereas the *egl-8*-null mutants *sa47* and *md1971* showed 0% and 18% larval growth arrest, respectively (Table 1). The *unc-73* RhoGEF-null mutants also took twice as long as the *egl-8* nulls to grow from newly hatched larvae to adults

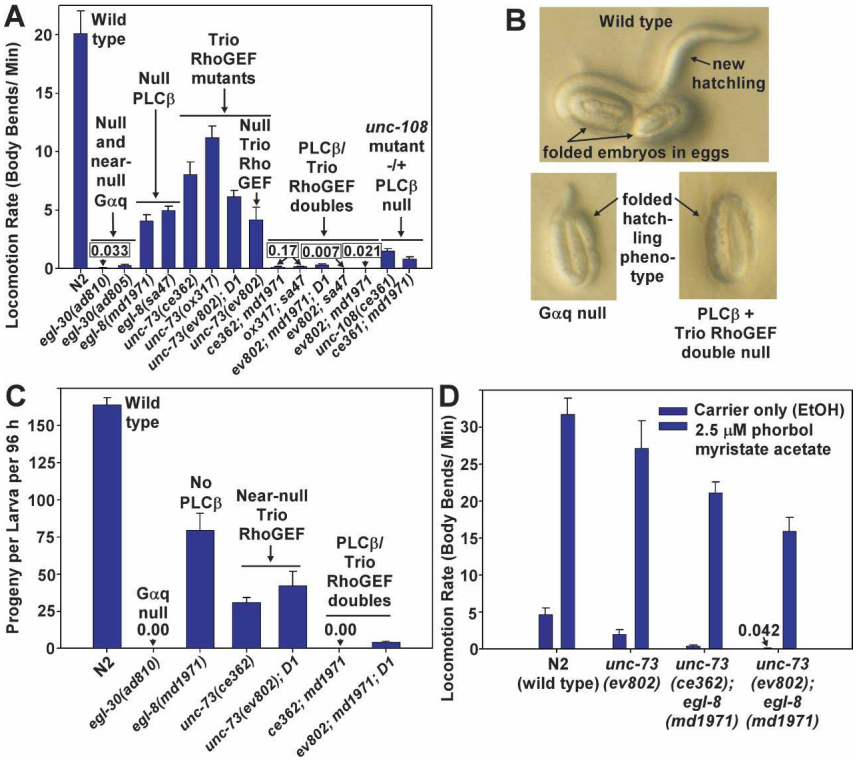

Figure 6. Double mutants containing null or near-null mutations for both EGL-8 (PLCβ) and UNC-73 RhoGEF domain phenocopy $G\alpha_q$-null mutants. (*A*) *egl-8* (PLCβ) and *unc-73* RhoGEF mutants show a synthetic interaction for locomotion. The graph shows mean locomotion rates of the indicated strains. Error bars are the standard errors of 10–12 animals. The *egl-30* and *egl-8* mutations used here are early stop codons, except for *egl-30(ad805)*, which is a splice site mutation (Brundage et al. 1996; Lackner et al. 1999; Miller et al. 1999). See also the Supplementary Movies. (*B*) $G\alpha_q$ and PLCβ/Trio RhoGEF-null mutants share the folded-hatchling phenotype. (*Top* panel) Photographs of a newly hatched wild-type larva next to two unhatched eggs containing late-stage folded embryos. (*Bottom* panels) Due to lack of locomotion, newly hatched mutant larvae remain folded as they were in the egg for hours after hatching. Genotypes of mutants are *egl-30(ad810)* (*bottom left*) and *unc-73(ev802); egl-8(md1971)* (*bottom right*). For scale, *C. elegans* eggs are ~50 μm in the long axis. See also the Supplementary Movies. (*C*) The synthetic interaction involves growth as well as locomotion. Shown are the mean growth rates of the indicated strains. Growth rate is measured as the mean number of progeny produced per animal over a 96-h period. Note that the growth rates of PLCβ/UNC-73 RhoGEF double mutants resemble the $G\alpha_q$ null and are much more severe than either single mutant. Error bars are the standard errors of three populations of larvae. (*D*) Phorbol esters rescue the paralysis of PLCβ/Trio Rho GEF double null mutants. Locomotion rates of wild type and the indicated mutants after 2 h of exposure to carrier (ethanol) or phorbol ester in ethanol. Data are means and standard errors of eight animals using 6-min locomotion assays. See also the Supplementary Movies.

Table 1. *Larval arrest in* unc-73; egl-8 *double mutants*

Genotype	Percentage larval arrest	Time range needed to reach adulthood for nonarrested animals (days of growth at 20°C)[a]
egl-8(md1971) null	17.8 ± 6.5%	2–4 d
egl-8(sa47) null	0.0 ± 0.0%	2–3 d
unc-73(ce362)	0.0 ± 0.0%	2–5 d
unc-73(ev802) RhoGEF null	54.0 ± 4.3%	4–7 d
unc-73(ev802); egl-8(md1971) double null	100.0 ± 0.0%[b]	N.A.
unc-73(ev802); egl-8(sa47) double null	100.0 ± 0.0%[b]	N.A.
egl-30(ad810) null	100.0% (*N* = 33 in one population)[b,c]	N.A.

Gravid adults were picked to culture plates and allowed to lay eggs for 16 h. Twenty of the youngest larvae from the hatched eggs on the plate were transferred to each of three locomotion plates and monitored twice a day over the next 10 d. Double mutants containing *ev802* were derived from *dpy-5(e61)* balanced heterozygotes (see strain list in Materials and Methods) and identified based on their *egl-30*-null-like phenotype. Data are the means and standard errors of three populations of 20 animals each. (N.A.) Not applicable.
[a]Time range covering first and last animals to reach adulthood of the 60 animals being followed for each strain.
[b]None of these animals grew past the mid-larval stage.
[c]Data are reprinted from Reynolds et al. (2005) with permission and are shown here for comparison.

(Table 1). A synthetic interaction for growth is also evident in nonnull allelic combinations of *unc-73 RhoGEF; egl-8* double mutants, which exhibit strongly reduced growth rates relative to each single mutant (Fig. 6C).

A previous study found that the DAG analog phorbol myristate acetate (PMA), if mixed in the right dosage into the media of culture plates, could restore wild-type levels of locomotion to $G\alpha_q$-null mutants within 2 h (Reynolds et al. 2005). If the double null mutants are essentially the same as $G\alpha_q$-null mutants, then we should also be able to rescue their paralysis with PMA, and that is indeed the case. Within 2 h of transferring the double null mutants to a plate containing 2.5 µM PMA, their locomotion rate improved ~360-fold, to a level greater than that of wild-type animals on control plates containing carrier only (Fig. 6D; Supplementary Movies). It is not clear whether the rescuing effects of PMA are due solely to overactivation of the PLCβ effector branch, thus compensating for lack of a Trio RhoGEF effector branch, or whether the Trio RhoGEF effector branch ultimately regulates DAG levels as well.

The synthetic interaction of PLCβ and UNC-73 RhoGEF nulls involved the egg-laying behavior as well as growth and locomotion. In *C. elegans*, the egg-laying rate can be quantified independent of growth rate by assessing the developmental stages of the eggs that are laid (Jose et al. 2007). Animals with high egg-laying rates lay early-stage eggs with eight or fewer cells rather than retaining the eggs in the uterus until the ~50- to 100-cell stage as wild type does (Jose and Koelle 2005). Animals with low egg-laying rates lay eggs in which embryos have developed to later stages, such as the comma, twofold, or threefold stages. Extremely low egg-laying rates result in internal hatching and a "bag-of-worms" phenotype caused by the hatchlings consuming the parent. We found that an *egl-8* (PLCβ) null showed a reduced egg-laying rate, but it was not nearly as severe as an *egl-30* ($G\alpha_q$) strong reduction-of-function mutant. Specifically, *egl-8(md1971)* laid 5% of its eggs at the two- or threefold stage compared with 50% for *egl-30(ad805)*. Furthermore, 0% of *egl-8* nulls had died of bag-of-worms within 48 h of reaching adulthood compared with 41% for *egl-30(ad805)* (Table 2). These result confirm that there is a missing $G\alpha_q$ effector for egg laying, as others had inferred (Bastiani et al. 2003). Our data show that Trio's RhoGEF domain plays a more critical role in egg laying than PLCβ, since 93% of the eggs laid by the *ev802* UNC-73 RhoGEF-null mutant are laid at the two- or threefold stage (Table 2). UNC-73 RhoGEF appears to be involved in $G\alpha_q$ signaling during egg laying because *unc-73* RhoGEF mutations strongly suppress the hyperactive egg laying of mutants with an overactive $G\alpha_q$ pathway (Table 2). We therefore quantified the egg-laying rate of *unc-73; egl-8* doubles to test for a synthetic interaction. Since the double null is larval arrested and thus cannot produce eggs, we assayed the nonnull *unc-73(ce362)* mutation in combination with an *egl-8* null. This double mutant showed a synthetic effect on egg laying. Whereas *egl-8*-null and *unc-73(ce362)* single mutants laid 5% and 62% of their eggs at the two- or threefold stage, respectively, the double mutant laid 98% of its eggs at these late stages (Table 2). In addition, 100% of the double mutants died of bag-of-worms within 48 h of reaching adulthood, whereas 0% and 8% of the *egl-8*-null and *unc-73(ce362)* single mutants, respectively, died of internal hatching (Table 2). A previous study found that mutations affecting UNC-73's Rac-specific GEF domain cause the bag-of-worms phenotype due to defective migration of the vulval precursor cells (Spencer et al. 2001). However, the bag-of-worms phenotype that we observed results from functional, not developmental, defects because phorbol esters restored egg laying in the double mutant to approximately wild-type levels within 2.5 h (Table 2).

In summary, the results in Figure 6 and Table 2 are consistent with PLCβ and Trio's Rho-specific GEF domain acting in separate pathways that together mediate the $G\alpha_q$ signaling that drives the locomotion, growth,

Table 2. *UNC-73 RhoGEF and PLCβ pathways interact to drive egg laying*

Genotype	Eggs laid at various developmental stages (percentage of total)						
	Eight or fewer cells	Eight to 50 cells	50 pregastrulation	Comma	Twofold	Threefold	Percentage of parents dying by internal hatching[a]
N2 (wild)	6.8 ± 1.2	44.8 ± 4.5	48.4 ± 4.0	0.0 ± 0.0	0.0 ± 0.0	0.0 ± 0.0	0.0 ± 0.0
egl-8(md1971)	0.0 ± 0.0	3.3 ± 0.61	86.5 ± 3.4	5.1 ± 0.90	3.7 ± 2.6	1.0 ± 1.4	0.0 ± 0.0
egl-30(ad805)	0.0 ± 0.0	0.0 ± 0.0	19.2 ± 3.5	30.9 ± 4.0	21.3 ± 3.5	28.7 ± 2.2	41.3 ± 12.7
goa-1(sa734)	92.8 ± 1.3	6.8 ± 1.4	0.0 ± 0.0	0.0 ± 0.0	0.0 ± 0.0	0.0 ± 0.0	0.0 ± 0.0
unc-73(ev802)	0.0 ± 0.0	0.0 ± 0.0	3.0 ± 1.7	3.0 ± 1.6	13.2 ± 2.0	80.3 ± 4.4	15.1 ± 4.2
unc-73(ce362)	0.0 ± 0.0	0.0 ± 0.0	13.8 ± 2.6	24.4 ± 7.9	18.2 ± 1.7	43.5 ± 11.3	8.3 ± 8.3
unc-73(ce362) goa-1(sa734)	0.0 ± 0.0	2.3 ± 0.37	72.6 ± 4.3	19.1 ± 2.9	4.5 ± 1.2	1.5 ± 0.29	20.8 ± 15.0
unc-73(ce362); egl-8(md1971)	0.0 ± 0.0	0.0 ± 0.0	1.2 ± 1.2	1.0 ± 1.0	15.9 ± .0	81.9 ± 4.9	100 ± 0.0
unc-73(ce362); egl-8(md1971) + 5 μM PMA[b]	3.4 ± 1.8	12.6 ± 3.8	58.5 ± 8.9	16.6 ± 6.3	8.3 ± 2.1	1.0 ± 0.7	0.0 ± 0.0

Data are means ± standard errors from three populations of day 1 adults, with each population averaging ≥100 eggs (i.e., ~300 eggs total among the three populations), except *unc-73(ce362); egl-8(md1971)*, which averaged 30 eggs per population for untreated animals (91 eggs total) and 40 eggs per population for the PMA-treated animals (121 eggs total).

[a]Scored 48 h after plating animals as day 1 adults. The total number of adults plated is as follows (in order of the strain list): three populations of four, six, 12, 15, 20, eight, eight, 20, and 15 animals each, respectively. The total number of adults present on all three plates at the time of scoring for internal hatching is as follows (in order of the strain list): 12, 18, 30, 42, 51, 55, and 31.

[b]PMA was included on the three trial plates for this strain. After a 2.5-h equilibration on the PMA plates, we removed all eggs that had been laid during the initial response to PMA and assayed all subsequently laid eggs.

and egg laying of the animal. Our data show that the Trio RhoGEF pathway is the dominant pathway for driving growth and egg laying, whereas the two pathways make about equal contributions in driving the locomotion behavior.

UNC-73E binds in a stable complex with activated EGL-30 ($G\alpha_q$)

If, as the above results suggest, UNC-73's RhoGEF domain is part of a $G\alpha_q$ effector pathway, $G\alpha_q$ might physically interact with the RhoGEF domain to cause RhoA activation, just as $G\alpha_q$ physically interacts with PLCβ to activate its phospholipase activity. Alternatively, $G\alpha_q$'s activation of RhoA could be indirect; i.e., mediated by $G\alpha_q$ signaling through one or more upstream proteins. However, our results argue against the latter possibility because we found that activated $G\alpha_q$ can physically associate with a stable complex containing UNC-73E when activated EGL-30 ($G\alpha_q$) and Flag-tagged UNC-73E are expressed together in human embryonic kidney (HEK293) cells, as determined by coimmunoprecipitation experiments (Fig. 7). This suggests that, in a cellular environment, activated *C. elegans* $G\alpha_q$ and UNC-73E (Trio RhoGEF) have a close physical interaction that mirrors their close genetic interaction in living animals.

Human Trio and UNC-73E enhance the activation of RhoA by EGL-30 ($G\alpha_q$)

To test whether Trio, and specifically the Rho-specific GEF domain of Trio, can mediate activation of RhoA by $G\alpha_q$, we transfected various combinations of activated Gα and Trio cDNAs into HEK293 cells and assayed for RhoA activation using two different assays. In the first assay, we monitored RhoA activation in intact cells using a reporter that produces luciferase in response to Rho-dependent transcription driven by the serum response element (SRE) promoter coupled to a luciferase cDNA (Mao et al. 1998; Lutz et al. 2004). In different experiments, we transfected four Trio constructs into the cells: (1) a full-length version of human Trio; (2) a

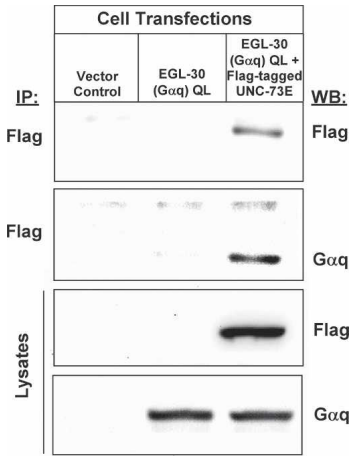

Figure 7. Activated EGL-30 ($G\alpha_q$) coimmunoprecipitates in a stable complex with UNC-73E (Trio RhoGEF) when coexpressed in HEK293 cells. HEK293 cells were transfected with 1 μg of *unc-73E* cDNA, 1 μg of activated *egl-30* ($G\alpha_q$ Q205L), and up to 2 μg of empty control vector. N-terminally Flag-tagged UNC-73E was precipitated with 2 μg of monoclonal Flag-M2 antibody and was analyzed by probing a Western blot with a Flag antibody or a specific $G\alpha_{q/11}$ antibody. The *bottom* panel shows expression levels of UNC-73E and EGL-30 ($G\alpha_q$ Q205L) in 20 μg of cell lysates.

fragment of human Trio consisting mainly of the Rho-specific GEF domain (Trio RhoGEF); (3) a full-length *unc-73e* cDNA; and (4) a fragment of *unc-73e* consisting mainly of the Rho-specific GEF domain (UNC-73E RhoGEF) (Fig. 8A). In cells lacking exogenous $G\alpha_q$ cDNA, the longer Trio constructs stimulated a weak basal level of luciferase production, which suggests that Trio is a very inefficient RhoGEF in the absence of an activator protein (Fig. 8B). The shorter constructs exhibited an even lower basal GEF activity (Fig. 8B). Cells transfected with constitutively active EGL-30 ($G\alpha_q$) Q205L showed a basal stimulation of RhoA activity due to the presence of an endogenous Trio-like protein that the cells express (Lutz et al. 2005). Upon coexpression with the various Trio proteins, the luciferase production induced by activated EGL-30 ($G\alpha_q$) was enhanced in a synergistic manner (Fig. 8B). Although the *unc-73e* construct had the strongest effect in this assay (~3.3-fold enhancement), full-length human Trio and the shorter RhoGEF domain constructs also caused synergistic luciferase production (approximately twofold enhancement) (Fig. 8B), which suggests that all of the Trio constructs enhance RhoA activation by activated EGL-30 ($G\alpha_q$). Because we isolated two of our *unc-73* suppressor mutants as suppressors of a $G\alpha_o$-null mutant, we also performed the same set of transfections with activated GOA-1 ($G\alpha_o$) substituted for activated EGL-30 ($G\alpha_q$). Compared with the vector control, activated GOA-1 ($G\alpha_o$) did not induce luciferase production and also did not show the large cooperative enhancement elicited by coexpression of activated EGL-30 ($G\alpha_q$) and the Trio variants (Fig. 8B).

As a direct assay for RhoA activation, we assayed the amount of GTP-liganded RhoA induced by the various cDNAs using the RhoA-binding domain of rhotekin fused to GST to pull down activated RhoA-GTP (Ren and Schwartz 2000; Lutz et al. 2004). In this assay, expression of UNC-73E, EGL-30 ($G\alpha_q$) Q205L, and GOA-1 ($G\alpha_o$) Q205L alone caused only marginal increases in the level of RhoA-GTP, whereas coexpression of UNC-73E and EGL-30 ($G\alpha_q$) Q205L, but not coexpression of UNC-73E and GOA-1 ($G\alpha_o$) Q205L, resulted in strong activation of RhoA (Fig. 8C). Taken together, all of these results suggest that activated EGL-30 ($G\alpha_q$) can induce RhoA activation via stimulation of UNC-73E (Trio RhoGEF).

An unc-73 RhoGEF mutation impairs $G\alpha_q$-stimulated RhoA activation

The above data predict that the missense mutations recovered in our genetic screens should prevent or reduce $G\alpha_q$-stimulated RhoA activation. To test this, we first analyzed the effect of the *unc-73(ce362)* mutation, which is the strongest missense mutation, on RhoA activation in intact cells using the luciferase reporter system described above. Although the mutant UNC-73E was expressed at levels similar to wild-type UNC-73E, the mutant protein was nearly inactive in $G\alpha_q$-stimulated RhoA activation, since the level of luciferase production was similar to cells containing $G\alpha_q$ without exogenous UNC-73 RhoGEF (Fig. 9A).

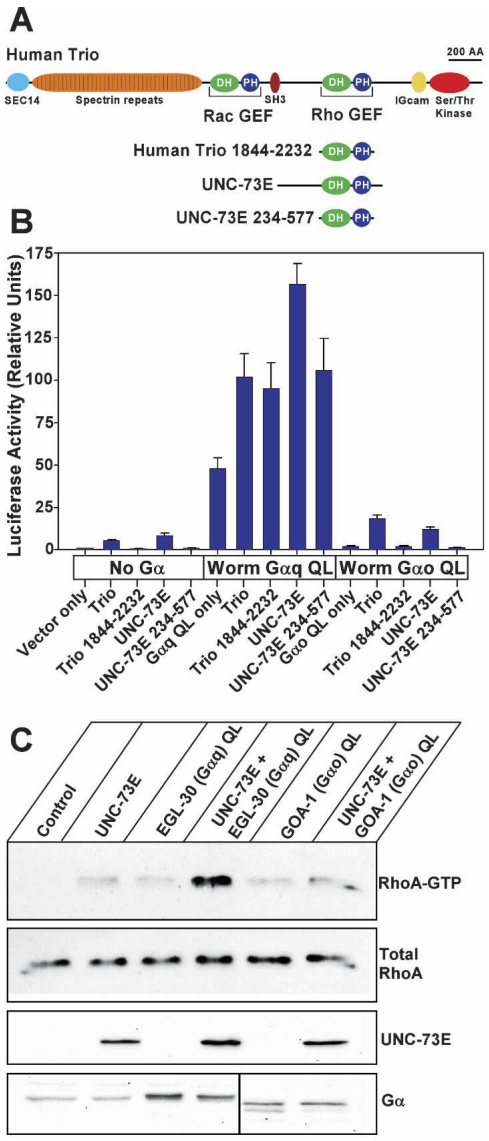

Figure 8. Activated EGL-30 ($G\alpha_q$), but not activated GOA-1 ($G\alpha_o$), synergizes with Trio and UNC-73E to activate RhoA in HEK293 cells. (*A*) Shown are the domain arrangements of the full-length and truncated Trio and *unc-73* cDNAs used for the cell transfection experiments. (*B*) Trio and UNC-73E enhance EGL-30 ($G\alpha_q$) Q205L-mediated SRE-driven transcription. The ability of *C. elegans* $G\alpha_q$ (Q205L) and $G\alpha_o$ (Q205L) to activate RhoA was tested in the presence or absence of Trio and UNC-73E expression using an assay that monitors Rho-dependent transcription of an SRE-controlled luciferase reporter gene. Data are the mean ratios of firefly/*Renilla* luciferase units ± standard errors ($n = 6$ transfections). (*C*) UNC-73E enhances RhoA activation in a Rho effector pull-down assay. RhoA activation was analyzed by a Rhotekin–Rho-binding domain pull-down assay. The amount of total RhoA as well as the expression levels of UNC-73E, EGL-30 ($G\alpha_q$ Q205L), and GOA-1 ($G\alpha_o$ Q205L) were analyzed in parallel using anti-RhoA-, anti-Flag-M2-, anti-$G\alpha_{q/11}$-, and anti-GOA-1 ($G\alpha_o$)-specific antibodies, respectively. Data are representative of duplicate independent experiments.

To gain molecular-level insights into the functions disrupted by the *ce362* mutation, we mapped the mutation onto the structure of the vertebrate $G\alpha_q$–p63RhoGEF–RhoA complex (Lutz et al. 2007) and then produced purified p63RhoGEF harboring the mutation to analyze its effects on the molecular activities of the complex. The residue mutated in *unc-73(ce362)* is conserved in human Trio and its paralogs, Kalirin/Duet and p63RhoGEF. The mutation is an Ile-to-Asn change of a solvent-exposed residue of the DH domain, on the surface opposite to the RhoA interaction site. In the structure, this isoleucine contributes to the interface with the C-terminal helix of $G\alpha_q$, and its substitution may also perturb local secondary structure in the region, which may also serve to lower affinity for the Gα subunit. Using purified proteins, we found that the *ce362* mutation decreases the basal RhoA nucleotide exchange activity [400 nM wild type activates nucleotide exchange on RhoA by 1.4 ± 0.1-fold (n = 12); 400 nM mutant activates by 1.1 ± 0.1-fold (n = 5)], lowers the affinity of $G\alpha_q$ binding by threefold (Fig. 9B), and also strongly impairs $G\alpha_q$-stimulated RhoA activation (Fig. 9C). When taken together with the cell-based RhoA activation data, these results are consistent with the *ce362* mutation strongly impairing the ability of $G\alpha_q$ to activate RhoA through Trio's Rho-specific GEF domain.

Discussion

In this study, we used two forward genetic screens to query the *C. elegans* genome for proteins important for $G\alpha_q$ signaling. By screening for mutants that suppress the phenotypes of an overactive $G\alpha_q$ pathway, both screens yielded mutations that specifically disrupt the RhoGEF domain of UNC-73 (Trio). Although the Rac-specific GEF domain in the longer isoforms of UNC-73 plays a prominent role in neuronal development (Steven et al. 1998), we used inducible and cell-specific promoters, as well as phorbol ester rescue experiments, to show that the Rho-specific GEF domain functions in adult neurons, after neuronal development is complete. In complementary genetic, biochemical, and cell-based experiments, we showed that Trio's Rho-specific GEF domain is a major $G\alpha_q$ effector that, together with PLCβ, mediates the $G\alpha_q$ signaling that drives the locomotion, egg laying, and growth of the animal. These results add important insights to an emerging body of evidence linking $G\alpha_q$-coupled receptors or activated $G\alpha_q$ to RhoA signaling.

Specifically, they identify the primordial $G\alpha_q$ effector whose duplication and divergence led to the Trio RhoGEF family of $G\alpha_q$ effectors, and they show that the Trio RhoGEF effector pathway can be as important as, or even more important than (for example, in driving growth and

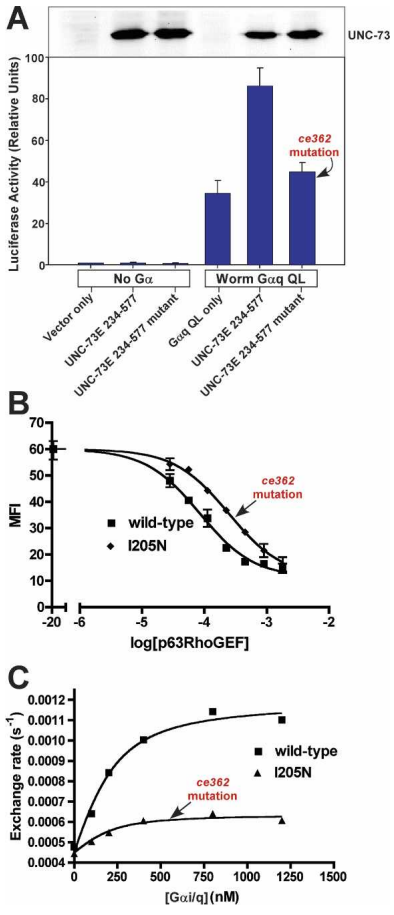

Figure 9. An UNC-73 RhoGEF mutation strongly impairs $G\alpha_q$-stimulated RhoA activation in cells and purified proteins. (*A*) The *unc-73(ce362)* mutation severely impairs $G\alpha_q$-stimulated RhoA activation in intact cells. The ability of *C. elegans* $G\alpha_q$ (Q205L) to activate RhoA was tested in the presence of wild-type or mutant UNC-73E 234–577 (*ce362* allele) using an assay that monitors Rho-dependent transcription of an SRE-controlled luciferase reporter gene. The *inset* at the *top* of the graph shows the expression levels of wild-type and mutant UNC-73 proteins, with lanes corresponding to the graph bars. Note that the mutant protein stimulates luciferase production only slightly more than $G\alpha_q$ alone, which exerts its effects through an endogenous Trio RhoGEF expressed in these cells. Data are the mean ratios of firefly/*Renilla* luciferase units ± standard errors (n = 4 transfections). (*B*) p63RhoGEF-I205N (the *ce362* mutation reproduced on p63RhoGEF) binds $G\alpha_q$ with threefold lower affinity. One representative competition experiment is shown, wherein increasing concentrations of unlabeled wild-type p63RhoGEF (residues 149–502) and its I205N mutant were mixed with 100 nM of fluor-labeled p63RhoGEF, and then incubated with $G\alpha_q$ immobilized on microspheres. Bead-associated fluorescence is reported as the median fluorescence intensity (MFI) for each concentration of protein, measured in duplicate. Calculated K_is (assuming K_d = 50 nM for fluor-labeled p63RhoGEF) were 30 ± 4 nM and 100 ± 9 nM for wild type and I205N, respectively. The $G\alpha_q$ used in this experiment is the $G\alpha_{i/q}$ chimera reported in Tesmer et al. (2005). (*C*) p63RhoGEF-I205N is impaired in its activation by $G\alpha_q$. Shown is a representative experiment. RhoA exchange activity was measured by fluorescence polarization. The calculated K_d (which assumes that the increase in rate is entirely due to the association of p63RhoGEF with $G\alpha_q$) is 90 ± 25 nM and 70 ± 35 nM for wild type and the I205N mutant, respectively. The $G\alpha_q$ used in this experiment is the $G\alpha_{i/q}$ chimera reported in Tesmer et al. (2005).

egg laying in *C. elegans*), the canonical PLCβ effector pathway in mediating $G\alpha_q$ signaling in living animals.

Genetic, biochemical, and structural approaches converge to identify Trio's Rho-specific GEF domain as a major, evolutionarily conserved $G\alpha_q$ effector

Interestingly, the ability of the Rho-specific GEF domain of Trio to function independently as a $G\alpha_q$ effector has been evolutionarily conserved. Like *C. elegans*, humans make splice variants of Trio that lack the Rac-specific GEF domain but contain the RhoGEF domain (Portales-Casamar et al. 2006). In addition, two paralogs, Kalirin/Duet and p63RhoGEF, are found in the human genome (Souchet et al. 2002; Lutz et al. 2004), of which Duet and p63RhoGEF exclusively contain the Rho-specific GEF domain. Of these, p63RhoGEF was the first RhoGEF shown to be physically and specifically coupled to activation by $G\alpha_q$ (Lutz et al. 2005). However, these observations have now been extended to the RhoGEF domains of human Trio and Kalirinin/Duet (Lutz et al. 2007; Rojas et al. 2007). These studies used purified proteins to show that activated $G\alpha_q$ directly interacts with the RhoGEF at specific sites, and that activated $G\alpha_q$ and the RhoGEF domain are sufficient to drive RhoA nucleotide exchange (Lutz et al. 2007; Rojas et al. 2007). The recently solved crystal structure of the $G\alpha_q$–p63RhoGEF–RhoA complex revealed that $G\alpha_q$ interacts with the DH/PH motifs of the GEF domain in a manner expected to relieve autoinhibition of the catalytic DH domain by the accessory PH domain, with the C-terminal tail of the PH domain docking into the $G\alpha_q$ effector-binding site and the C-terminal region of $G\alpha_q$ binding the DH domain (Lutz et al. 2007). Unlike vertebrates, *C. elegans* has only one Trio ortholog (UNC-73) and produces domain diversity in Trio proteins by alternative promoters and splicing. Thus the primordial $G\alpha_q$ effector was most likely a Trio ortholog that underwent duplication to produce the paralogs p63RhoGEF and Kalirin/Duet, which may allow for specialized $G\alpha_q$ effector functions and/or sites of expression in vertebrates. This interpretation of conserved $G\alpha_q$ effector function is further supported by the finding that the *unc-73(ce362)* and *unc-73(ox322)* mutations map either directly in or are predicted to be disruptive of the p63RhoGEF DH and PH domain interfaces with $G\alpha_q$ (Lutz et al. 2007), and, as shown in this study, the *ce362* mutation disrupts the ability of $G\alpha_q$ to activate p63RhoGEF. Thus, complementary approaches ranging from the genetics of living animals down to the structure of molecular complexes have converged on an important conclusion: The Rho-specific GEF domain that is found in the Trio family of proteins is a major, evolutionarily conserved, direct effector of $G\alpha_q$.

The PLCβ and RhoA effector pathways are both important for $G\alpha_q$ signaling in living animals

Can the two $G\alpha_q$ effector pathways act in the same cells, or do some cell types predominantly use one of the pathways? Evidence from previous *C. elegans* studies suggests that both scenarios exist. For example, both *egl-30* ($G\alpha_q$) and some *unc-73* RhoGEF-containing isoforms are expressed in the vulval muscles that mediate egg laying and in the pharynx (Bastiani et al. 2003; Steven et al. 2005). UNC-73 RhoGEF has also been shown to function in the pharynx (Steven et al. 2005). In contrast, *egl-8* (PLCβ) seems to be absent or below detection limits in the vulval muscles and pharynx (Lackner et al. 1999; Miller et al. 1999). However, there do not seem to be any tissues that express both *egl-30* ($G\alpha_q$) and *egl-8* (PLCβ) but not *unc-73* (Trio RhoGEF), and all three proteins are strongly expressed together throughout the nervous system (Lackner et al. 1999; Miller et al. 1999; Bastiani et al. 2003; Steven et al. 2005). *egl-8* is also expressed without *unc-73* (Trio RhoGEF) or *egl-30* ($G\alpha_q$) in the posterior intestine, where it regulates a $G\alpha_q$-independent posterior body wall muscle contraction during defecation (Lackner et al. 1999; Miller et al. 1999). The close correspondence between $G\alpha_q$ and Trio RhoGEF expression in various tissues, the apparent lack of PLCβ expression in some $G\alpha_q$-expressing cells, and our finding that the Trio RhoGEF pathway is the dominant pathway for driving growth and egg laying raise the interesting possibility that Trio's Rho-specific GEF domain may be the primordial $G\alpha_q$ effector, and that PLCβ may have been coopted as an additional $G\alpha_q$ effector for specific cell types at a later point in evolution. However, the recently completed draft sequence of the *Nematostella* sea anemone genome (Putnam et al. 2007) revealed orthologs (defined as reciprocal best-scoring BLAST hits) of all three proteins ($G\alpha_q$, PLCβ, and Trio) (data not shown). Thus $G\alpha_q$, orthologs of which are not found outside the animal kingdom, may already have been signaling through both PLCβ and Trio in the last common cnidarian-bilaterian animal ancestor, which lived an estimated 670–820 million years ago (Putnam et al. 2007). Although this underscores the ancient origin of the pathway, further clues of its evolutionary history will have to await the forthcoming genomes of even simpler animals and animal precursors, such as sponges, placozoans, and choanoflagellates.

In *C. elegans*, both EGL-8 (PLCβ) and UNC-73 RhoGEF function in the nervous system to drive the locomotion behavior, and knocking out either effector results in similarly sluggish locomotion. Thus, both effector pathways make similarly important contributions to locomotion. Given that $G\alpha_q$ and both of its effectors are broadly expressed in the nervous system, we speculate that, in many neurons, $G\alpha_q$ may activate both pathways in the same cell. Previous studies provided evidence that EGL-30 ($G\alpha_q$), EGL-8 (PLCβ), and RHO-1 (RhoA) control locomotion and neurotransmitter release by acting in the cholinergic motor neurons that are the final link between synaptic transmission and the locomotion behavior (Lackner et al. 1999; McMullan et al. 2006). These findings, coupled with the finding that some of the UNC-73 RhoGEF isoforms (such as UNC-73E) are strongly expressed in both head and motor neurons (Steven et al. 2005), suggest that both effector pathways can function in the same neurons. However, we

have been unable to directly demonstrate that UNC-73 RhoGEF functions in motor neurons. Indeed, expression of UNC-73E under control of a motor neuron promoter had no effect on the sluggish locomotion phenotype of *unc-73(ce362)* (data not shown), whereas expression under a pan-neuronal promoter gave full rescue (i.e., Fig. 4B). This suggests that UNC-73 RhoGEF is required in other neurons as well as motor neurons or, less likely, that it is only required in nonmotor neurons.

Other sources of RhoA activation in regulating synaptic signaling

Biochemical and structural studies in vertebrates have clearly shown that $G\alpha_{12}/G\alpha_{13}$ functions as a major activator of RhoA through its direct interactions with the RGS domain of p115RhoGEF (Hart et al. 1998; Katoh et al. 1998; Wells et al. 2002). Previous *C. elegans* studies also identified GPA-12 ($G\alpha_{12}$) as an activator of p115 RhoGEF and RHO-1 (RhoA) (Yau et al. 2003; Hiley et al. 2006). Hyperactivating this pathway, which is broadly expressed in *C. elegans* neurons, increases aldicarb sensitivity and causes exaggerated body movements through its effects on inhibiting DGK-1 (diacylglycerol kinase), to which RHO-1 directly binds (Hiley et al. 2006; McMullan et al. 2006). However, deletions of GPA-12 or p115 RhoGEF have no obvious effect on locomotion rate or aldicarb sensitivity (Hiley et al. 2006), which indicates that one or more other RhoA activators contribute to the sluggish phenotype and aldicarb resistance of animals expressing the Rho inactivator C3 transferase (Hiley et al. 2006; McMullan et al. 2006). The sluggish phenotype of animals lacking UNC-73 RhoGEF is consistent with UNC-73-activated RHO-1 being a major target in C3 transferase-induced sluggishness. However, the relatively mild aldicarb sensitivity of *unc-73* RhoGEF mutants (this study) compared with animals expressing C3 transferase (McMullan et al. 2006) suggests that other RhoA activation pathways may contribute to synaptic signaling in *C. elegans*.

Materials and methods

Forward genetic screens

For the *egl-8(md1971)* enhancer screen, we EMS-mutagenized *egl-8(md1971); ceEx149* (*rab-3::egl-8* cDNA/rab-3::GFP) L4-stage animals and produced synchronous F2 adult grandprogeny of the mutagenized animals. We then plated a single animal carrying the GFP-marked array on each of 2000 solid-media culture wells on 24-well plates and incubated the plates for 4 d at room temperature to produce the F3 generation. The *ceEx149* extrachromosomal array rescued the sluggish locomotion of *egl-8*-null mutants and transmitted the array to ~60% of its progeny. We therefore screened the plates for wells in which all of the animals that had lost the rescuing array were arrested as *egl-30*-null-like paralyzed larvae, or for wells in which the arrayless animals appeared synthetically paralyzed relative to their array-containing siblings in the well. We repeated the screen for 13 weekly cycles for a total of 26,000 F2s plated, which is approximately threefold knockout coverage for the genome. For the *goa-1(sa734)* suppressor screen, we mutagenized L4-stage *goa-1* mutants with 1 mM ENU dissolved in ethanol (De Stasio and Dorman 2001). *goa-1(sa734)* is a null mutant with an early stop codon (Robatzek and Thomas 2000). We produced synchronous F2 grandprogeny of the mutagenized animals and plated these animals as young larvae on 24-well culture plates using a repeat pipetter to plate ~100 animals in each well for a total of 50,000 animals. We screened both the F2 and F3 generations on these plates, but had the most success in screening the F3 generation, which involved growing the cultures for 2 d at room temperature and 4 d at 20°C after plating. We screened the wells for mutants with improved growth and reduced hyperactive behaviors, including both locomotion and egg laying. We identified the *unc-73(ce367) goa-1(sa734)* double mutant on our *goa-1(sa734)* stock plates as a spontaneous suppressor with a strong growth advantage over *goa-1(sa734)* single mutants. For the *egl-30(tg26)* suppressor screen, we mutagenized young adult *egl-30(tg26)* animals with 0.5 mM ENU and picked them in groups of five to 20 animals to 6-cm agar plates. The F1 progeny were washed off after laying eggs, and the semisynchronous F2 broods were screened for improved growth and reduced hyperactivity. Approximately 18,000 haploid mutagenized genomes were screened. *egl-30(tg26)* contained the R243Q mutation that decreases GTP hydrolysis and results in a dominant hyperactive locomotion and slow-growth phenotype (Doi and Iwasaki 2002; Natochin and Artemyev 2003; Reynolds et al. 2005).

Mapping, identification, and outcrossing of suppressor mutations

Before mapping the new suppressor mutations, we separated the mutations from *goa-1(sa734)* or *egl-30(tg26)* by crossing N2 males to the suppressed strain and isolating putative suppressor single mutants in the F2 generation based on their predicted sluggish phenotype. Animals that were both homozygous for the mutation and did not segregate *goa-1(sa734)* or *egl-30(tg26)* were kept as 1× outcrossed strain stocks. In the case of the *unc-73(ce362)* allele, we produced an *unc-73(ce362); dpy-11(e224)* double mutant for use in complementation tests and a 3× outcrossed version of the mutant that we then used to make the final 5× outcrossed versions of *unc-73(ce362)* and *unc-73(ce362) goa-1(sa734)*. In the course of outcrossing *ce362*, we found tight linkage to *goa-1* on Chromosome I. We then mapped the mutation relative to single-nucleotide polymorphisms (SNPs) using methods similar to those described previously (Schade et al. 2005) to further narrow the location to a region centered around –1.8 on Chromosome I that included the *unc-73* gene. Complementation tests revealed that the sluggish phenotype of *unc-73(ce362)* partially noncomplemented *unc-73(e936)*, whereas *ce362* and *ce367* fully noncomplemented each other and *unc-73(ev802)*. PCR and sequencing of the *unc-73* gene in our mutants revealed mutations in the Rho-specific GEF domain. *ox317* and *ox322* failed to complement each other and were mapped with SNPs (Davis et al. 2005) to an interval on Chromosome I slightly left of cosmid E01A2 (–1.66) and very close to cosmid F28H1 (–1.87). Fine mapping was aided by picking Dpy non-Unc and Unc non-Dpy recombinants from *ox317 dpy-5(e61)*/CB4856. *ox317*-complemented *unc-73(e936)*, but failed to complement *unc-73(ev802)*, and sequencing confirmed that *ox317* and *ox322* carried mutations in the Rho-GEF domain of *unc-73*.

Live animal assays

For larval arrest assays, we picked gravid adults to culture plates and allowed them to lay eggs for 16 h. We then transferred 20 of the youngest larvae from the hatched eggs on the plate to each

of three locomotion plates and monitored them twice a day over the next 10 d, picking off any animals that had matured to adults, eggs that had been laid, or larvae that had died during each 12-h period. Larvae that died by desiccation after crawling off of the media or unaccounted/missing larvae were not included in the final numbers. We used these same plates to quantify the number of *unc-73(ev802); egl-8(md1971)* double mutants that remained alive after 10 d. Death was defined as absence of stimulated movement in the tip of the nose when prodded with a platinum pick, accompanied by the appearance of partial decomposition. For growth rate assays, we plated a predetermined number of L1 larvae on each of three growth assay plates (see "Worm Strains and Culture" in the Supplemental Material) and incubated them for 96 h at 20°C. The number of L1 larvae per plate was strain-specific and based on estimates of the growth rate and the number needed to produce ~300–500 progeny over the 96 h. For strains with wild-type growth, we plated four L1 larvae per plate. We then counted the F1 progeny (eggs and larvae) and normalized the data to progeny per animal plated. We performed standard locomotion assays as described (Miller et al. 1999; Reynolds et al. 2005). For strains with 100% larval arrest [*egl-30(ad810)* and doubles with *unc-73(ev802)*], we collected 6- to 30-h-old larval-arrested animals as progeny of balanced heterozygotes (see the Strain list in the Supplemental Material) and identical stage controls of N2 (wild type) as described for other larval-arrested strains (Reynolds et al. 2005). For all locomotion assays using larvae, we counted body bends for a single 6-min period for each of 10–15 animals that had been freshly plated on standard locomotion plates and stabilized 2–4 h before assaying. We performed locomotion assays of phorbol ester-treated animals as described (Reynolds et al. 2005), using 5 µM PMA and a 2.5-h time point for *unc-73(ce362); egl-8(md1971)* adults and 2.5 µM PMA with the following time points for assays using larvae: 1.0 h (N2), 1.5 h [*unc-73(ev802)*], 2 h [*unc-73(ev802); egl-8(md1971)*]. We performed heat-shock locomotion assays as described (Schade et al. 2005). For egg-laying assays, we aged animals 15 h from the mid-L4 or young adult stage (the latter if the strain was very slow growing), and then distributed equal numbers (the exact number plated was strain-specific) to each of three spot plates (made by spotting 6 µL of OP-50 bacteria to an unseeded plate and growing for 24 h at room temperature). We then scanned the spot of bacteria hourly [or every 30 min for wild type, PMA-treated strains, and *goa-1(sa734)*] for up to 9 h or until ~300 eggs (100 per trial plate) had been laid in the bacteria and counted. After noting the developmental stage of each egg laid during the preceding time interval, we picked all eggs off of the bacteria. We preincubated PMA-treated strains on 5 µM PMA assay plates for 4–5 h, and then picked off the eggs that had been laid during the preincubation before beginning the first 30-min interval. This allowed sufficient time for the PMA to induce laying of the late-stage eggs that were in the uterus before PMA exposure and that would otherwise bias the early time points of the assay. We used a 2.5× objective (225× magnification) to assess the stage of each egg, and a 1.2× objective with a longer working distance to pick off eggs after each time point. After the assay, we saved the plates and noted the number of animals that died over the next 48 h due to internal hatching. We performed aldicarb and levamisole paralysis assays as described (Charlie et al. 2006b). We captured and converted videos of worms on culture plates as described (Schade et al. 2005).

Double mutants

We constructed double mutants using the standard method of crossing heterozygous males of mutant A with homozygous hermaphrodites of mutant B and cloning virgin F1 cross-progeny. From plates segregating mutant A in their F2 progeny, we cloned mutant A or B animals and looked for segregation of the double mutant in the next generation. To facilitate identification of some *unc-73; egl-8* and *unc-108; egl-8* double mutant combinations, we marked *egl-8* mutants with the *dpy-5(e61)* mutation such that the crosses placed the *dpy-5* mutation in *trans* to the closely linked *unc-73* or *unc-108*. This allowed us to identify animals homozygous for the desired chromosome, or to identify balanced *unc-73(ev802)* heterozygotes for making *unc-73(ev802); egl-8* loss-of-function doubles. The homozygosity of the *unc-73(ce362); egl-8(md1971)* double mutant was verified by PCR and sequencing. We made *unc-73(ev802); egl-8(md1971); qaIs7312* using similar methods, except that we used a pan-neuronal GFP marker in *qaIs7312* to follow the array.

Cell culture and transfection

Human embryonic kidney cells (HEK293) were maintained in high-glucose Dulbecco's modified Eagle's medium (DMEM) supplemented with 10% heat-inactivated fetal calf serum, 100 U/mL penicillin, 100 µg/mL streptomycin, and 2 mM glutamine at 37°C in an atmosphere of 5% CO_2. DNA transfections were performed with Polyfect (Qiagen) according to the manufacturer's recommendations in 96-well and six-well formats for measuring SRE activation and RhoA activation or protein interaction, respectively. After transfection, the cells were maintained in serum-reduced (0.5%) DMEM for 48 h.

Rho activity assays

To quantify Rho-dependent SRE activation, reporter gene assays were performed with the Dual Luciferase Reporter Assay System (Promega) according to the manufacturer's protocol as described previously (Mao et al. 1998; Lutz et al. 2004). In brief, HEK293 cells were seeded into 96-well plates and cotransfected with the indicated plasmids (30 ng of *C. elegans* Gα plasmids, 60 ng of the respective *unc-73*/Trio plasmids, and up to 90 ng of an empty control vector as indicated) together with the pSRE.L firefly luciferase reporter plasmid (21 ng; kindly provided by Dr J. Mao and Dr. D. Wu, University of Rochester, NY) and the pRL-TK (4 ng; Promega) *Renilla* luciferase control vector. Forty-eight hours after transfection, the cells were lysed with passive lysis buffer (Promega), and luciferase activities were determined with the Envision Instrument (Perkin Elmer) in a white 96-well plate. We also determined RhoA activation by a Rho effector pull-down assay as described previously (Ren and Schwartz 2000; Lutz et al. 2004). In brief, HEK293 cells were seeded in six-well plates and transfected with the respective plasmids (1.3 µg *unc-73e* plasmid in the absence or presence of 0.6 µg of the respective Gα plasmids and up to 2 µg of an empty control vector). Forty-eight hours after transfection, the cells were scraped off in a buffer containing 1% (v/v) Nonidet P40. The precleared lysates were incubated for 1 h on ice with 70 µg of purified GST-Rho-binding domain of Rhotekin bound to glutathione-Sepharose while continuously shaking. After three washing steps, the bound proteins were eluted with sample buffer and separated by 15% SDS-PAGE. RhoA was then detected by immunoblotting with a specific RhoA antibody (1 µg/mL; 26C4; Santa Cruz Biotechnology). The expression level of the proteins and exogenous RhoA was analyzed in 40 µg of the precleared lysates.

Immunoprecipitations

For coimmunoprecipitation of UNC-73E with different constitutively active Gα subunits, HEK293 cells were seeded in six-

well plates and transfected with the respective plasmids and up to 2 µg of an empty control vector. Forty-eight hours after transfection, the cells were lysed with 600 µL of immunoprecipitation buffer (10 mM Tris-HCl at pH 7.4, 150 mM NaCl, 0.1% Triton X-100, protease inhibitor tablets [Roche]) and homogenized for 30 sec. After centrifugation (26,000*g* for 10 min at 4°C), the supernatants were precleared with 40 µL of a 1:1 slurry of protein A Sepharose (GE Healthcare). Then, 2 µg of anti-Flag M2 antibody (Sigma-Aldrich) were added to each sample and incubated for 30 min on ice. After addition of 40 µL of equilibrated protein A Sepharose, the samples were gently shaken for 4 h at 4°C. After three washing steps, the bound proteins were eluted and denaturated with 25 µL of sample buffer for 5 min at 95°C. The precipitated proteins were analyzed by separating 10–40 µg of protein by discontinuous SDS-PAGE (10%–15% acrylamide) and transferring onto a nitrocellulose membrane. For detection of specific proteins, the following antibodies were used: anti-Flag-M2 antibody (1.0 µg/mL; Sigma-Aldrich) for detection of N-terminally Flag-tagged Trio, anti-RhoA antibody (1 µg/mL; 26C4; Santa Cruz Biotechnology), anti-$G\alpha_{q/11}$ antibody (0.2 µg/mL; C-19; Santa Cruz Biotechnology), and anti-GOA-1 antibody (gift of Michael Koelle, Yale University, New Haven, CT).

Biochemical analysis of the ce362 mutation

With the exception of the $G\alpha_{i/q}$ chimera, we expressed all of the proteins for this analysis in bacteria and purified them as described (Lutz et al. 2007). These included wild-type and mutant versions of p63RhoGEF (p63RhoGEF and p63RhoGEF-I205N, the latter of which contains the *ce362* mutation) and RhoA. We purified $G\alpha_{i/q}$ chimeras from insect cells as described (Tesmer et al. 2005). For the $G\alpha_q$-binding competition experiment, we mixed increasing concentrations of unlabeled wild-type p63RhoGEF (residues 149–502) and its I205N mutant with 100 nM p63RhoGEF labeled with Alexa-Fluor 532, and then incubated with $G\alpha_{i/q}$-linked *x*Map LumAvidin microspheres (Luminex) in 20 mM HEPES (pH 8.0), 100 mM NaCl, 5 mM $MgCl_2$, 0.1% lubrol, 5 mM DTT, 1% BSA, 20 µM $AlCl_3$, and 10 mM NaF. The bead-associated fluorescence was measured in a Luminex 96-well plate bead analyzer, in duplicate. Data were fit to a single site competition curve using GraphPad Prism. The K_d of fluor-labeled p63RhoGEF-I205N for $G\alpha_{i/q}$ is 96 ± 27 nM ($n = 3$), which is not significantly different from the K_d of the unlabeled mutant protein in Figure 9. We measured RhoA exchange activity by fluorescence polarization as described in a companion publication (Lutz et al. 2007). A one-phase exponential association curve with time lag was used to fit each curve, generated by mixing 2 µM RhoA with either 200 nM wild-type p63RhoGEF (residues 149–502) or the I205N mutant, and with increasing amounts of $G\alpha_{i/q}$, as indicated. In each individual experiment, curves were measured in triplicate, and their k_{app} values were fit simultaneously to single-phase exponential association curves in GraphPad Prism. The rate versus $G\alpha_{i/q}$ concentration was then fit to a saturation binding with ligand depletion curve (rate = $(B_{max}/[GEF]) * ((K_d + [GEF] + [G\alpha_{i/q}]) - \sqrt{((K_d + [GEF] + [G\alpha_{i/q}])^2 - (4 * [GEF] * [G\alpha_{i/q}]))}/2)$.

Acknowledgments

We thank Mark Lackner and Joshua Kaplan for providing the full-length *egl-8* cDNA KP309, Robert Steven for the *unc-73(ev802)*- containing strains, Michael Koelle for the GOA-1 antibody, and Aruna Shankaranarayanan for technical assistance. This work was supported by grants from the National Institutes of Health (NS034307 to E.J., HL086865 to J.J.G.T., and GM080765 to K.G.M.) and a grant from the Oklahoma Center for the Advancement of Science to K.G.M. (HR06-078). E.M.J. is an Investigator of the Howard Hughes Medical Institute. S.L. was supported by a junior research grant of the Medical Faculty Mannheim and M.A. by a fellowship from the Helen Hay Whitney Foundation.

References

Barnes, W.G., Reiter, E., Violin, J.D., Ren, X.R., Milligan, G., and Lefkowitz, R.J. 2005. β-Arrestin 1 and Gαq/11 coordinately activate RhoA and stress fiber formation following receptor stimulation. *J. Biol. Chem.* **280:** 8041–8050.

Bastiani, C.A., Gharib, S., Simon, M.I., and Sternberg, P.W. 2003. *Caenorhabditis elegans* $G\alpha_q$ regulates egg-laying behavior via a PLC_b-independent and serotonin-dependent signaling pathway and likely functions both in the nervous system and in muscle. *Genetics* **165:** 1805–1822.

Bourne, H.R. 1997. How receptors talk to trimeric G proteins. *Curr. Opin. Cell Biol.* **9:** 134–142.

Brundage, L., Avery, L., Katz, A., Kim, U., Mendel, J.E., Sternberg, P.W., and Simon, M.I. 1996. Mutations in a *C. elegans* $G_q\alpha$ gene disrupt movement, egg laying, and viability. *Neuron* **16:** 999–1009.

Charlie, N.K., Schade, M.A., Thomure, A.M., and Miller, K.G. 2006a. Presynaptic UNC-31 (CAPS) is Required to activate the $G\alpha_s$ pathway of the synaptic signaling network. *Genetics* **172:** 943–961.

Charlie, N.K., Thomure, A.M., Schade, M.A., and Miller, K.G. 2006b. The dunce cAMP phosphodisterase PDE-4 negatively regulates $G\alpha_s$-dependent and $G\alpha_s$-independent cAMP pools in the *Caenorhabditis elegans* synaptic signaling network. *Genetics* **173:** 111–130.

Chase, D.L., Patikoglou, G., and Koelle, M.R. 2001. Two RGS proteins that inhibit $G\alpha_o$ and $G\alpha_q$ signaling in *C. elegans* neurons require a Gβ5-like subunit for function. *Curr. Biol.* **11:** 222–231.

Chikumi, H., Vazquez-Prado, J., Servitja, J.M., Miyazaki, H., and Gutkind, J.S. 2002. Potent activation of RhoA by $G\alpha_q$ and G_q-coupled receptors. *J. Biol. Chem.* **277:** 27130–27134.

Davis, M.W., Hammarlund, M., Harrach, T., Hullett, P., Olsen, S., and Jorgensen, E.M. 2005. Rapid single nucleotide polymorphism mapping in *C. elegans*. *BMC Genomics* **6:** 118. doi: 10.1186/1471-2164-6-118.

Desai, C., Garriga, G., McIntire, S.L., and Horvitz, H.R. 1988. A genetic pathway for the development of the *Caenorhabditis elegans* HSN motor neurons. *Nature* **336:** 638–646.

De Stasio, E.A. and Dorman, S. 2001. Optimization of ENU mutagenesis of *Caenorhabditis elegans*. *Mutat. Res.* **495:** 81–88.

Doi, M. and Iwasaki, K. 2002. Regulation of retrograde signaling at neuromuscular junctions by the novel C2 domain protein AEX-1. *Neuron* **33:** 249–259.

Dutt, P., Kjoller, L., Giel, M., Hall, A., and Toksoz, D. 2002. Activated $G\alpha_q$ family members induce Rho GTPase activation and Rho-dependent actin filament assembly. *FEBS Lett.* **531:** 565–569.

Gally, C., Eimer, S., Richmond, J.E., and Bessereau, J.L. 2004. A transmembrane protein required for acetylcholine receptor clustering in *Caenorhabditis elegans*. *Nature* **431:** 578–582.

Gilman, A.G. 1987. G proteins: Transducers of receptor-generated signals. *Annu. Rev. Biochem.* **56:** 615–649.

Hajdu-Cronin, Y.M., Chen, W.J., Patikoglou, G., Koelle, M.R., and Sternberg, P.W. 1999. Antagonism between $G_o\alpha$ and $G_q\alpha$

in *C. elegans*: The RGS protein EAT-16 is necessary for $G_o\alpha$ signaling and regulates $G_q\alpha$ activity. *Genes & Dev.* **13:** 1780–1793.

Hart, M.J., Jiang, X., Kozasa, T., Roscoe, W., Singer, W.D., Gilman, A.G., Sternweis, P.C., and Bollag, G. 1998. Direct stimulation of the guanine nucleotide exchange activity of p115 RhoGEF by Gα13. *Science* **280:** 2112–2114.

Hedgecock, E.M., Culotti, J.G., Hall, D.H., and Stern, B.D. 1987. Genetics of cell and axon migrations in *Caenorhabditis elegans*. *Development* **100:** 365–382.

Hepler, J.R. and Gillman, A.G. 1992. G proteins. *Trends Biochem. Sci.* **17:** 383–387.

Hiley, E., McMullan, R., and Nurrish, S.J. 2006. The Gα12–RGS RhoGEF–RhoA signalling pathway regulates neurotransmitter release in *C. elegans*. *EMBO J.* **25:** 5884–5895.

Hubbard, K.B. and Hepler, J.R. 2006. Cell signalling diversity of the Gqα family of heterotrimeric G proteins. *Cell. Signal.* **18:** 135–150.

Jose, A.M. and Koelle, M.R. 2005. Domains, amino acid residues, and new isoforms of *Caenorhabditis elegans* diacylglycerol kinase 1 (DGK-1) important for terminating diacylglycerol signaling in vivo. *J. Biol. Chem.* **280:** 2730–2736.

Jose, A.M., Bany, I.A., Chase, D.L., and Koelle, M.R. 2007. A specific subset of transient receptor potential vanilloid-type channel subunits in *Caenorhabditis elegans* endocrine cells function as mixed heteromers to promote neurotransmitter release. *Genetics* **175:** 93–105.

Katoh, H., Aoki, J., Yamaguchi, Y., Kitano, Y., Ichikawa, A., and Negishi, M. 1998. Constitutively active Gα12, Gα13, and $G\alpha_q$ induce Rho-dependent neurite retraction through different signaling pathways. *J. Biol. Chem.* **273:** 28700–28707.

Koelle, M.R. and Horvitz, H.R. 1996. EGL-10 regulates G protein signaling in the *C. elegans* nervous system and shares a conserved domain with many mammalian proteins. *Cell* **84:** 112–125.

Lackner, M.R., Nurrish, S.J., and Kaplan, J.M. 1999. Facilitation of synaptic transmission by EGL-30 $G_q\alpha$ and EGL-8 PLCβ: DAG binding to UNC-13 is required to stimulate acetylcholine release. *Neuron* **24:** 335–346.

Liu, X., Wang, H., Eberstadt, M., Schnuchel, A., Olejniczak, E.T., Meadows, R.P., Schkeryantz, J.M., Janowick, D.A., Harlan, J.E., Harris, E.A., et al. 1998. NMR structure and mutagenesis of the N-terminal Dbl homology domain of the nucleotide exchange factor Trio. *Cell* **95:** 269–277.

Lutz, S., Freichel-Blomquist, A., Rumenapp, U., Schmidt, M., Jakobs, K.H., and Wieland, T. 2004. p63RhoGEF and GEFT are Rho-specific guanine nucleotide exchange factors encoded by the same gene. *Naunyn Schmiedebergs Arch. Pharmacol.* **369:** 540–546.

Lutz, S., Freichel-Blomquist, A., Yang, Y., Rumenapp, U., Jakobs, K.H., Schmidt, M., and Wieland, T. 2005. The guanine nucleotide exchange factor p63RhoGEF, a specific link between Gq/11-coupled receptor signaling and RhoA. *J. Biol. Chem.* **280:** 11134–11139.

Lutz, S., Shankaranarayanan, A., Coco, C., Ridilla, M., Nance, M., Vettel, C., Baltus, D., Evelyn, C., Neubig, R.R., Wieland, T., et al. 2007. Structure of the $G\alpha_q$–p63RhoGEF–RhoA complex reveals a conserved pathway for activation of RhoA by GPCRs. *Science* (in press).

Mao, J., Yuan, H., Xie, W., Simon, M.I., and Wu, D. 1998. Specific involvement of G proteins in regulation of serum response factor-mediated gene transcription by different receptors. *J. Biol. Chem.* **273:** 27118–27123.

McIntire, S.L., Garriga, G., White, J., Jacobson, D., and Horvitz, H.R. 1992. Genes necessary for directed axonal elongation or fasciculation in *C. elegans*. *Neuron* **8:** 307–322.

McMullan, R., Hiley, E., Morrison, P., and Nurrish, S.J. 2006. Rho is a presynaptic activator of neurotransmitter release at pre-existing synapses in *C. elegans*. *Genes & Dev.* **20:** 65–76.

Mendel, J.E., Korswagen, H.C., Liu, K.S., Hajdu-Cronin, Y.M., Simon, M.I., Plasterk, R.H.A., and Sternberg, P.W. 1995. Participation of the protein G_o in multiple aspects of behavior in *C. elegans*. *Nature* **267:** 1652–1655.

Miller, K.G., Alfonso, A., Nguyen, M., Crowell, J.A., Johnson, C.D., and Rand, J.B. 1996. A genetic selection for *Caenorhabditis elegans* synaptic transmission mutants. *Proc. Natl. Acad. Sci.* **93:** 12593–12598.

Miller, K.G., Emerson, M.D., and Rand, J.B. 1999. $G_o\alpha$ and diacylglycerol kinase negatively regulate the $G_q\alpha$ pathway in *C. elegans*. *Neuron* **24:** 323–333.

Miller, K.G., Emerson, M.D., McManus, J., and Rand, J.B. 2000. RIC-8 (synembryn): A novel conserved protein that is required for $G_q\alpha$ signaling in the *C. elegans* nervous system. *Neuron* **27:** 289–299.

Natochin, M. and Artemyev, N.O. 2003. A point mutation uncouples transducin-α from the photoreceptor RGS and effector proteins. *J. Neurochem.* **87:** 1262–1271.

Neer, E.J. 1995. Heterotrimeric G proteins: Organizers of transmembrane signals. *Cell* **80:** 249–257.

Nonet, M.L., Grundahl, K., Meyer, B., and Rand, J.B. 1993. Synaptic function is impaired but not eliminated in *C. elegans* mutants lacking synaptotagmin. *Cell* **73:** 1291–1305.

Nurrish, S., Segalat, L., and Kaplan, J.M. 1999. Serotonin inhibition of synaptic transmission: $G\alpha_o$ decreases the abundance of UNC-13 at release sites. *Neuron* **24:** 231–242.

Offermanns, S., Zhao, L.P., Gohla, A., Sarosi, I., Simon, M.I., and Wilkie, T.M. 1998. Embryonic cardiomyocyte hypoplasia and craniofacial defects in Gαq/Gα11-mutant mice. *EMBO J.* **17:** 4304–4312.

Portales-Casamar, E., Briancon-Marjollet, A., Fromont, S., Triboulet, R., and Debant, A. 2006. Identification of novel neuronal isoforms of the Rho-GEF Trio. *Biol. Cell.* **98:** 183–193.

Putnam, N.H., Srivastava, M., Hellsten, U., Dirks, B., Chapman, J., Salamov, A., Terry, A., Shapiro, H., Lindquist, E., Kapitonov, V.V., et al. 2007. Sea anemone genome reveals ancestral eumetazoan gene repertoire and genomic organization. *Science* **317:** 86–94.

Rand, J.B. and Nonet, M.L. 1997. Synaptic transmission. In *C. elegans II* (eds. D.H. Riddle et al.), pp. 611–643. Cold Spring Harbor Laboratory Press, Cold Spring Harbor, NY.

Ren, X.D. and Schwartz, M.A. 2000. Determination of GTP loading on Rho. *Methods Enzymol.* **325:** 264–272.

Reynolds, N.K., Schade, M.A., and Miller, K.G. 2005. Convergent, RIC-8 dependent Gα signaling pathways in the *C. elegans* synaptic signaling network. *Genetics* **169:** 650–670.

Richmond, J.E., Davis, W.S., and Jorgensen, E.M. 1999. UNC-13 is required for synaptic vesicle fusion in *C. elegans*. *Nat. Neurosci.* **2:** 959–964.

Richmond, J.E., Weimer, R.M., and Jorgensen, E.M. 2001. An open form of syntaxin bypasses the requirement for UNC-13 in vesicle priming. *Nature* **412:** 338–341.

Robatzek, M. and Thomas, J.H. 2000. Calcium/calmodulin-dependent protein kinase II regulates *Caenorhabditis elegans* locomotion in concert with a G_o/G_q signaling network. *Genetics* **156:** 1069–1082.

Robatzek, M., Niacaris, T., Steger, K., Avery, L., and Thomas, J.H. 2001. *eat-11* encodes GPB-2, a $G\beta_5$ ortholog that interacts with $G_o\alpha$ and $G_q\alpha$ to regulate *C. elegans* behavior. *Curr. Biol.* **11:** 288–293.

Rojas, R.J., Yohe, M.E., Gershburg, S., Kawano, T., Kozasa, T., and Sondek, J. 2007. $G\alpha_q$ directly activates p63RhoGEF and Trio via a conserved extension of the DH-associated PH do-

main. *J. Biol. Chem.* doi: 10.1074/jbc.M703458200.
Schade, M.A., Reynolds, N.K., Dollins, C.M., and Miller, K.G. 2005. Mutations that rescue the paralysis of *C. elegans ric-8* (Synembryn) mutants activate the $G\alpha_s$ pathway and define a third major branch of the synaptic signaling network. *Genetics* **169:** 631–649.
Segalat, L., Elkes, D.A., and Kaplan, J.M. 1995. Modulation of serotonin-controlled behaviors by G_o in *Caenorhabditis elegans. Nature* **267:** 1648–1651.
Siddiqui, S.S. 1990. Mutations affecting axonal growth and guidance of motor neurons and mechanosensory neurons in the nematode *Caenorhabditis elegans. Neurosci. Res. Suppl.* **13:** S171–S190. doi: 10.1016/0921-8696(90)90047-7.
Siddiqui, S.S. and Culotti, J.G. 1991. Examination of neurons in wild type and mutants of *Caenorhabditis elegans* using antibodies to horseradish peroxidase. *J. Neurogenet.* **7:** 193–211.
Smrcka, A.V., Hepler, J.R., Brown, K.O., and Sternweis, P.C. 1991. Regulation of polyphosphoinositide-specific phospholipase C activity by purified Gq. *Science* **251:** 804–807.
Souchet, M., Portales-Casamar, E., Mazurais, D., Schmidt, S., Leger, I., Javre, J.L., Robert, P., Berrebi-Bertrand, I., Bril, A., Gout, B., et al. 2002. Human p63RhoGEF, a novel RhoA-specific guanine nucleotide exchange factor, is localized in cardiac sarcomere. *J. Cell Sci.* **115:** 629–640.
Spencer, A.G., Orita, S., Malone, C.J., and Han, M. 2001. A RHO GTPase-mediated pathway is required during P cell migration in *Caenorhabditis elegans. Proc. Natl. Acad. Sci.* **98:** 13132–13137.
Steven, R., Kubiseski, T.J., Zheng, H., Kulkarni, S., Mancillas, J., Ruiz Morales, A., Hogue, C.W., Pawson, T., and Culotti, J. 1998. UNC-73 activates the Rac GTPase and is required for cell and growth cone migrations in *C. elegans. Cell* **92:** 785–795.
Steven, R., Zhang, L., Culotti, J., and Pawson, T. 2005. The UNC-73/Trio RhoGEF-2 domain is required in separate isoforms for the regulation of pharynx pumping and normal neurotransmission in *C. elegans. Genes & Dev.* **19:** 2016–2029.
Taylor, S.J., Chae, H.Z., Rhee, S.G., and Exton, J.H. 1991. Activation of the β 1 isozyme of phospholipase C by α subunits of the Gq class of G proteins. *Nature* **350:** 516–518.
Tesmer, V.M., Kawano, T., Shankaranarayanan, A., Kozasa, T., and Tesmer, J.J. 2005. Snapshot of activated G proteins at the membrane: The $G\alpha q$–GRK2–$G\beta\gamma$ complex. *Science* **310:** 1686–1690.
van der Linden, A.M., Simmer, F., Cuppen, E., and Plasterk, R.H. 2001. The G protein β-subunit GPB-2 in *Caenorhabditis elegans* regulates the $G_o\alpha$–$G_q\alpha$ signaling network through interactions with the regulator of G protein signaling proteins EGL-10 and EAT-16. *Genetics* **158:** 221–235.
Vogt, S., Grosse, R., Schultz, G., and Offermanns, S. 2003. Receptor-dependent RhoA activation in G12/G13-deficient cells: Genetic evidence for an involvement of Gq/G11. *J. Biol. Chem.* **278:** 28743–28749.
Wells, C.D., Liu, M.Y., Jackson, M., Gutowski, S., Sternweis, P.M., Rothstein, J.D., Kozasa, T., and Sternweis, P.C. 2002. Mechanisms for reversible regulation between G13 and Rho exchange factors. *J. Biol. Chem.* **277:** 1174–1181.
Wightman, B., Baran, R., and Garriga, G. 1997. Genes that guide growth cones along the *C. elegans* ventral nerve cord. *Development* **124:** 2571–2580.
Wilkie, T.M., Scherle, P.A., Strathmann, M.P., Slepak, V.Z., and Simon, M.I. 1991. Characterization of G protein α subunits in the Gq class: Expression in murine tissues and in stromal and hematopoietic cell lines. *Proc. Natl. Acad. Sci.* **88:** 10049–10053.
Yau, D.M., Yokoyama, N., Goshima, Y., Siddiqui, Z.K., Siddiqui, S.S., and Kozasa, T. 2003. Identification and molecular characterization of the G α12-Rho guanine nucleotide exchange factor pathway in *Caenorhabditis elegans*. *Proc. Natl. Acad. Sci.* **100:** 14748–14753.